Korean J. Chem. Eng., **16**(4), 449-455 (1999)

Synthesis and Electrochemical Characterization of $LiMn_2O_4$ Cathode Materials for Lithium Polymer Batteries

Yang-Kook Sun† and Dong-Won Kim

Polymer Materials Laboratory, Chemical Sector, Samsung Advanced Institute of Technology, 103-12, Moonji-Dong, Yusong-Gu, Taejon 305-380, Korea

(Received 30 November 1998 • accepted 12 May 1999)

Abstract–Spinel $LiMn_2O_4$ powders with sub-micron, narrow particle-size distribution, and phase-pure particles were synthesized at low temperatures from aqueous solution of metal acetate containing glyoxylic acid as a chelating agent by a sol-gel method. The effects of the calcination temperature and glyoxylic acid quantity on the physicochemical properties of spinel $LiMn_2O_4$ powders were examined with X-ray diffractometry (XRD), the Brunauer-Emmett-Teller (BET) method and scanning electron microscopy (SEM). Porous $LiMn_2O_4$ electrode was characterized electrochemically with charge/discharge experiments and A.C. impedance spectroscopy. The cycling performance of a Li/polymer electrolyte/$LiMn_2O_4$ cell has been discussed in terms of contact and interfacial resistance by A. C. impedance spectroscopy.

Key words : Lithium Manganese Oxide, Sol-Gel Method, Chelating Agent, Glyoxylic Acid, Lithium Polymer Batteries

INTRODUCTION

Lithium polymer batteries are now being studied extensively as a promising source for electric vehicles and portable electronic equipment. The use of polymer electrolyte would make the batteries safe, flexible, light, and thin. One of the problems with lithium polymer batteries is a progressive capacity fading with repeated cycling. When polymer electrolyte is used, the establishment of a proper interfacial contact between polymer electrolyte and electrode can be an issue of major concern. Many studies have been carried out in order to investigate the interfacial characteristics between polymer electrolyte and electrode [Steele et al., 1983; Bruce et al., 1989; Ratnakumar et al., 1989; Koksbang et al., 1991]. The A.C. impedance method is a useful tool for the characterization of composite electrode/electrolyte interfacial properties, especially in three electrode cells including a reference electrode. The technique has been previously used to investigate the interfacial properties of the lithium metal/solid polymer electrolyte [Hiratani et al., 1988; Fauteux, 1988] and the composite cathode/electrolyte (liquid and solid polymer) interface [Steele et al., 1983; Ratnakumar et al., 1989; Koksbang et al., 1991]. It was reported that the capacity fading with repeated cycling was related to the change of composite cathode/polymer electrolyte interface and morphology in the composite cathode rather than the reduction of the extent of the intercalation process [Koksbang et al., 1991].

Considerable efforts have been devoted to the synthesis and characterization of spinel $LiMn_2O_4$ and its application for lithium secondary batteries since it is easier to prepare, cheaper and less toxic than the layered oxides such as $LiCoO_2$ and $LiNiO_2$ [Maclin et al., 1991; Guyomard et al., 1994]. The quality of $LiMn_2O_4$ powders used in lithium secondary batteries strongly depends on its synthetic method [Gao et al., 1996]. Recently, one of the authors has reported that spinel $LiMn_2O_4$ powders with phase-pure particles could be synthesized by the sol-gel method using Poly (acrylic acid) (PAA) and glycolic acid as chelating agent [Sun et al., 1997; Sun, 1997].

In this work, $LiMn_2O_4$ powders were synthesized by a sol-gel method using glyoxylic acid as a chelating agent at considerably lower temperatures and short processing time. The cycling performance of Li/polymer electrolyte/$LiMn_2O_4$ cell was evaluated, and the capacity fading during cycling was studied in terms of interfacial characteristics with A.C. impedance measurements.

EXPERIMENTAL

$LiMn_2O_4$ powders were prepared according to the procedure shown in Fig. 1. A stoichiometric amount of Li and Mn acetate (Acros Co., high purity) salts with the cationic ratio of Li : Mn = 1 : 2 was dissolved in distilled water and mixed well with an aqueous solution of glyoxylic acid (Aldrich, high purity). Glyoxylic acid was used as a chelating agent to produce gel. Ammonium hydroxide was added slowly to this solution with a constant stirring until a pH of 4-6 was achieved. The resultant solution was evaporated at 70-80 °C for 5 hr until a transparent sol was obtained. To remove water, the sol was heated at 70-80 °C while being mechanically stirred. As the evaporation of water proceeded, the sol turned into a viscous transparent gel. For the preparation of the gel precursors with different molar ratio of glyoxylic acid to total metal ions, the same procedure was repeated with the molar ratio of glyoxylic acid to total metal ions being varied to 1, 2, and 2.5. The resulting gel precursors were decomposed at 250-800 °C for 10 hr in air to obtain phase-pure polycrystalline $LiMn_2O_4$ powders.

†To whom correspondence should be addressed.
E-mail : yksun@sait.samsung.co.kr

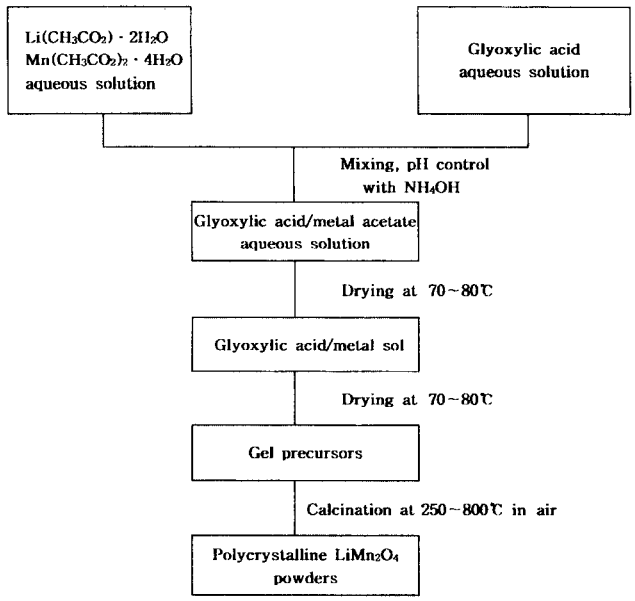

Fig. 1. Flowsheet of the procedure preparing polycrystalline $LiMn_2O_4$ powders by the glyoxylic acid-assisted sol-gel method.

Powder X-ray diffraction (Rint-2000, Rigaku) using CuK_α radiation was used to identify the crystallinity of the materials calcined at various temperatures. Rietveld refinement was then performed on the X-ray diffraction data to obtain the lattice constants. The morphological changes of the powders were observed by using a field emission scanning electron microscope (Hitachi Co., S-4100). The specific surface area of the material was determined by the BET method (Autosorb-1, Quantachrome) with nitrogen adsorption.

The electrochemical properties of $LiMn_2O_4$ powders were determined in Li/polymer electrolyte/$LiMn_2O_4$ cells. The polymer electrolyte was made from poly(acrylonitrile) (PAN), plasticized by a solution of $LiClO_4$ in a 1 : 1 mixture of ethylene carbonate (EC) and propylene carbonate (PC). A typical polymer electrolyte composition was PAN 12 wt%-EC 40 wt%-PC 40 wt%- $LiClO_4$ 8 wt%. The ionic conductivity of polymer electrolyte was $2\times10^{-3}\ \Omega^{-1}\,cm^{-1}$ at room temperature. The composite cathode was made from $LiMn_2O_4$ spinel powders (89.5 wt%), acetylene black (5.5 wt%), and PAN binder (5 wt%). The $LiMn_2O_4$ spinel powders and acetylene black were added to PAN solution in dimethyl sulfoxide (DMSO) as a solvent. The slurry was spread onto an Al foil current collector, and dried at 110 °C in air. The dried composite cathode was then compressed with roll presser and further dried under vacuum for >10 hr at 110 °C. A three-electrode cell was used for the electrochemical measurements. The reference and counter electrodes consisted of 50 μm thick Li foil (Cyprus Foote Mineral Co.) pressed onto Cu current collectors. A rechargeable lithium polymer cell was assembled by sandwiching the polymer electrolyte between the Li anode and composite cathode, and then the reference electrode was placed on the composite cathode side. The cell was then enclosed in a metallized plastic bag and vacuum sealed. All assemblies of the cell were carried out in a dry box filled with Ar. The cells were usually cycled between cut-off voltages of 3.4 and 4.3 V at a constant current density of 0.15 mA/cm^2, unless otherwise noted. The cells were activated by first cycle at a constant current density of 0.10 mA/cm^2. A.C. impedance measurements were performed using a Zahner Elektrik IM6 impedance analyzer over the frequency range of 1 mHz-100 kHz with an amplitude of 5 mV_{rms}. Each sample was allowed to equilibrate for 30 min at each cycle before the measurement at the fully charged state.

RESULTS AND DISCUSSION

The transparent gel could be formed for all of the ratios of glyoxylic acid to total metal ions tested in this study. The transparent gel precursors with uniform color proved to be homogeneous. It is believed that the carboxylic groups on the glyoxylic acid could form chemical bonds with the metal ions and these mixtures became extremely viscous polymeric resins as they were gelled [Lessing, 1989].

Fig. 2 shows the X-ray diffraction (XRD) patterns of the $LiMn_2O_4$ powders calcined at various temperatures for 10 hr in air, where the molar ratio of glyoxylic acid to total metal ions was 2.0. The materials calcined at 200 °C were amorphous with no diffraction peaks. However, after the temperature was increased to 250 °C, poorly crystalline $LiMn_2O_4$ spinel phase was formed. Impurity peaks, such as Li_2CO_3 and $MnCO_3$, were not observed, which are often found in other low-temperature techniques. The diffraction peaks become much sharper with a shift toward the low-angle side in the XRD pattern when the calcination temperature was increased. This result indicates a gradual growth of average particle size and an increase in crystallinity of the $LiMn_2O_4$ powders. It is inferred from the above results that since the cross-linked gel precursors may provide more homogeneous mixing of the cations and less tendency for segregation during calcination though the chemical bonding is destroyed, the use of glyoxylic acid as a chelating agent greatly suppresses the formation of precipitates from which the hetero-

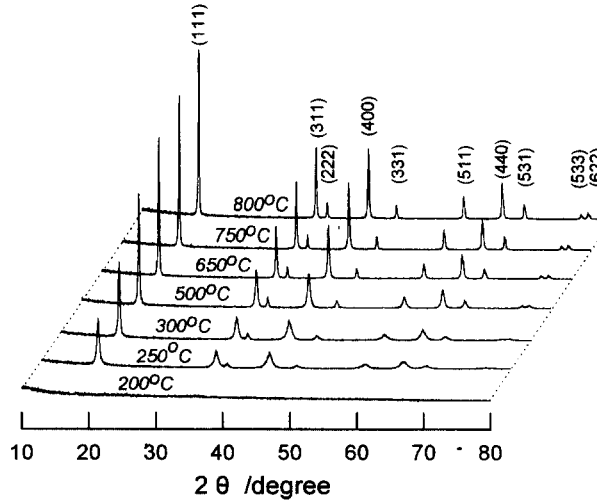

Fig. 2. X-ray diffraction patterns of gel derived materials calcined at various temperatures when the molar ratio of glyoxylic acid to total metal ions was 2.0.

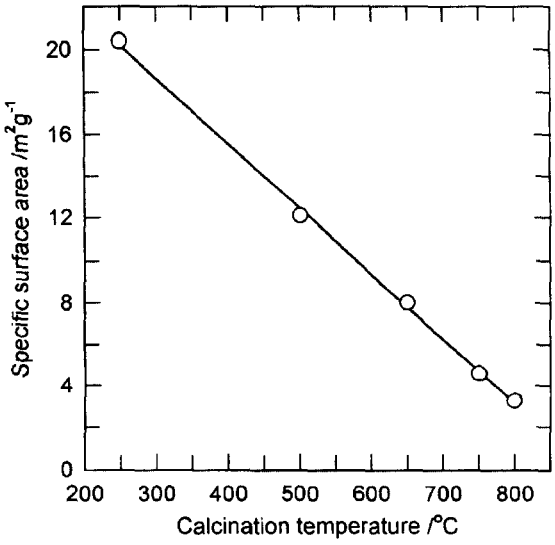

Fig. 3. Effect of the calcination temperature on the specific surface area of $LiMn_2O_4$ powders when the molar ratio of glyoxylic acid to total metal ions was 2.0.

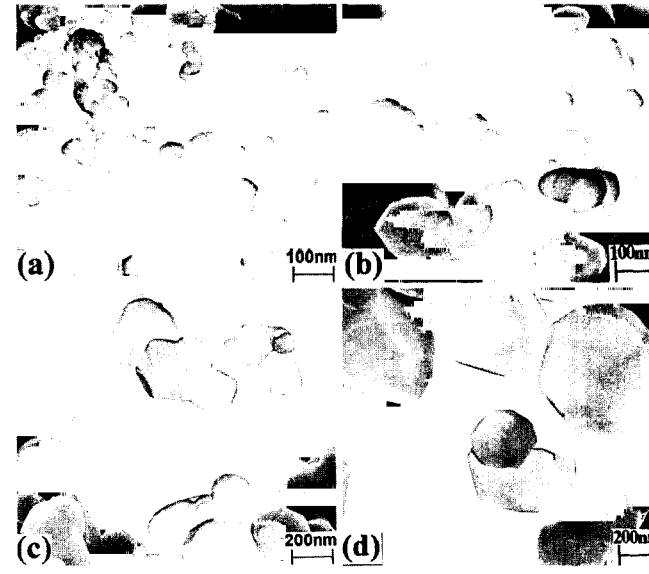

Fig. 5. Scanning electron micrographs of the $LiMn_2O_4$ powders calcined at (a) 300, (b) 650, (c) 750, and (d) 800 °C.

geneity stems. Subsequently, the fine mixture state of the cations in the homogeneous composition oxidized to form crystallites of phase-pure spinel $LiMn_2O_4$ powders under the mild conditions. Similar results have been reported where $LiMn_2O_4$ powders were synthesized through the sol-gel method [Sun et al., 1997; Sun, 1997].

Fig. 3 shows the effect of the calcination temperature on the specific surface area of the same materials as shown in Fig. 2. The specific surface area of the $LiMn_2O_4$ powders decreases linearly with increasing calcination temperature, due to the growth of $LiMn_2O_4$ crystallites. The specific surface area was determined to be 20.4 m^2/g and 3.3 m^2/g for the material calcined at 250 °C and 800 °C, respectively.

Fig. 4 shows the effect of the calcination temperature on the

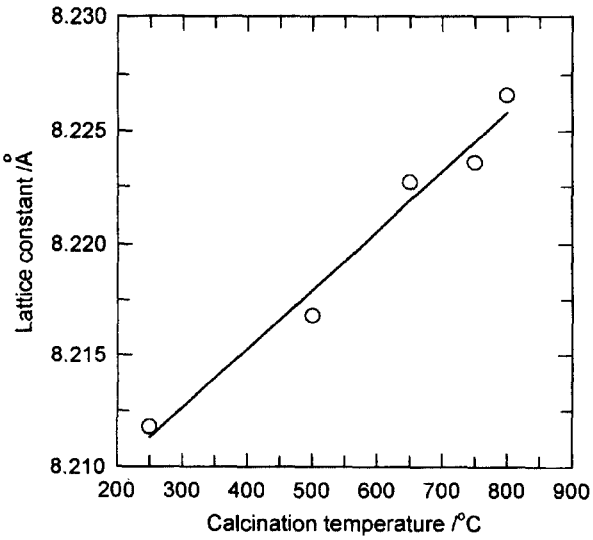

Fig. 4. Effect of the calcination temperature on the lattice constant of the $LiMn_2O_4$ powders when the molar ratio of glyoxylic acid to total metal ions was 2.0.

lattice constant a, obtained from the Rietveld refinement on the XRD data of the same materials as shown in Fig. 2. The lattice constant increases almost linearly up to 8.227 Å with increasing calcination temperature from 250 to 800 °C. It is speculated that the value of the average oxidation state of manganese in the spinel phase is closely related to the lattice constant of the cubic unit cell. Lower calcination temperature results in the formation of more-oxidized Mn cations because Mn ions are stable preferentially as Mn^{4+} at lower temperatures [Masquelier et al., 1996]. For example, MnO_2 with all Mn^{4+} transforms progressively to Mn_2O_3 with all Mn^{3+} for the binary manganese oxide system as the temperature increases. The atomic radius of Mn^{4+} (0.67 Å) is smaller than that of Mn^{3+} (0.72 Å) and thus the lattice constant of the cubic unit cell of the spinel $LiMn_2O_4$ calcined at higher temperatures is larger than that of these calcined at lower temperatures.

Fig. 5 shows scanning electron micrographs (SEM) for the $LiMn_2O_4$ powders calcined the gel precursors of the molar ratio of glyoxylic acid to metal ions of 2.0 at various temperature for 10 hr in air. The presence of loosely agglomerated spherical particles with average grain size of 40 nm was observed for the powders calcined at 300 °C. As calcination temperature was increased, growth kinetics were favored and thus agglomerated spherical particles were changed to a larger particulate. For the materials calcined at 650 °C, the particle size increased to 100 nm. When the gel precursors were heated at 750 °C, the particle size of the particulates increased to about 300 nm with a fairly narrow particle-size distribution. For the materials calcined at 800 °C, the particle sizes of the particulates abruptly increased to about 600 nm with a narrow particle-size distribution.

In order to investigate the effect of glyoxylic acid quantity on the morphological features of $LiMn_2O_4$ powders, scanning electron microscopy (SEM) was used for the powders prepared from the gel precursors having a molar ratio of glyoxylic acid to metal ions of 2.5 and 1.0, and calcined at 700 °C for 10 hr in

Fig. 6. Scanning electron micrographs for the $LiMn_2O_4$ powders calcined at 700 °C when the molar ratio of glyoxylic acid to metal ions was (a) 2.5 and (b) 1.0.

air as shown in Fig. 6. The surface of the powders with a molar ratio of glyoxylic acid to total metal ions of 2.5 contained monodispersed spherical fine particulates with an average particle size of about 100 nm. For the powders with a molar ratio of glyoxylic acid to total metal ions of 1.0, it was observed that the particle size of the powders was 200 nm. The particle size of the former was two times smaller than the latter at the same calcination temperature.

The reason why the particle size of the $LiMn_2O_4$ powders decreases with the glyoxylic acid quantity used can be explained as follows. The less the glyoxylic acid used in preparaing gel precursors, the shorter is distance between Li and Mn cations, and thus the higher is the probability of the crystallization between the cations. Therefore, bigger particles will be produced at the less glyoxylic acid quantity. On the contrary, when the glyoxylic acid quantity is increased, the highly cross-linked gel precursors suppress the cation mobility and effectively prevent the cations from contacting each other. Thus, the degree of segregation of the cations during calcination is decreased, and the homogeneously distributed cations are crystallized into the spinel phase with the increase of calcination temperature ; thus the particles do not grow in size.

From the above results, we concluded that $LiMn_2O_4$ powders with a wide variety of physicochemical properties such as particle size, crystallity, specific surface area, and microcrystallite morphologies could be controlled by simply varying the pyrolysis processing and chelating agent quantity.

Fig. 7 represents the charge/discharge curves of the Li/polymer electrolyte/$LiMn_2O_4$ cell at the discharge current densities of 0.1 to 1.0 mA/cm^2. In this cell, the composite cathode was prepared from the $LiMn_2O_4$ powders calcined at 800 °C. The cell was charged to 4.3 V at constant current density of 0.1 mA/cm^2 before each discharge. The cell delivered a capacity of more than 130 mAh/g at a current densities of 0.1, 0.2, and 0.3 mA/cm^2. The discharge capacity of the cell decreased very slowly with the increase of current density. For example, at current

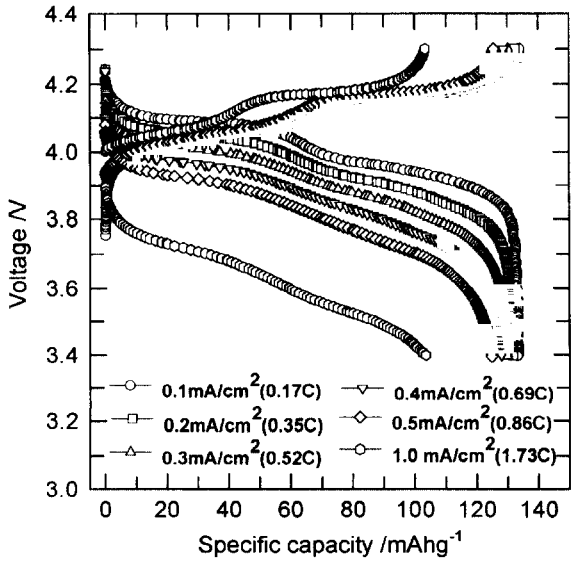

Fig. 7. Charge/discharge curves at various discharge current densities for Li/polymer electrolyte/$LiMn_2O_4$ cells. The cell was charged to 4.3 V at 0.1 mA/cm^2 before each discharge.

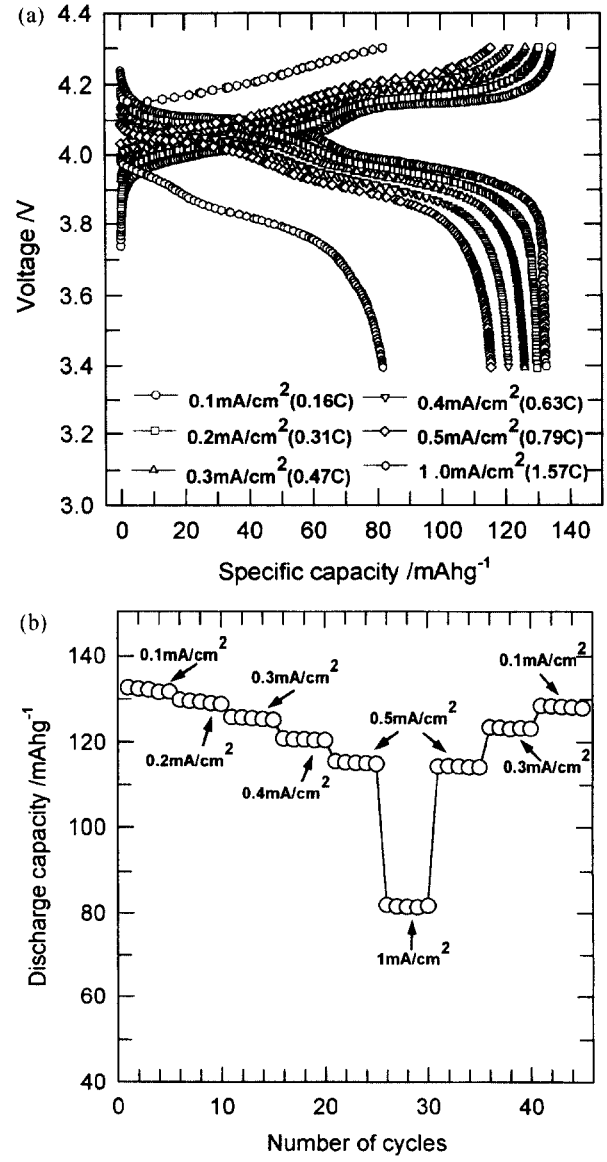

Fig. 8. (a) Charge/discharge curves and (b) variation of specific discharge capacity with number of cycles for the Li/polymer electrolyte/$LiMn_2O_4$ cells at various current densities.

density of 0.5 mA/cm^2 or 0.86 C rate, the discharge capacity was 125 mAh/g. This cell showed an attractive capacity of 104 mAh/g at current density 1 mA/cm^2 or 1.73 C rate. However, the cell polarization (half of the difference in voltage between the charge and discharge curves) increased as the discharge current density increased.

Fig. 8 shows the charge/discharge curves and the variation of the discharge capacities with the number of cycles for the Li/polymer electrolyte/$LiMn_2O_4$ cell using $LiMn_2O_4$ powders calcined at 800 °C. Various charge/discharge current densities were applied progressively with cycling. The cell showed excellent capacity retention at all current densities. The discharge capacities of the cell slowly decreased with increasing current densities and were determined to be 133, 130, 126, 121, and 116 mAh/g at current densities of 0.1, 0.2, 0.3, 0.4, and 0.5 mA/cm^2, respectively. By further increasing of the current density to 1 mA/cm^2 or 1.57 C rate, the discharge capacity abruptly drops to 82 mAh/g and stabilizes during the following four cycles. After current densities of 0.5, 0.3, and 0.1 mA/cm^2 at the 31, 36, 41th cycle were applied, the discharge capacities increased to 114, 124, and 128 mAh/g, respectively. The observed cycling stability of the spinel $LiMn_2O_4$ could be due to a small structural transition in the material and good contacts among the composite cathode constituents.

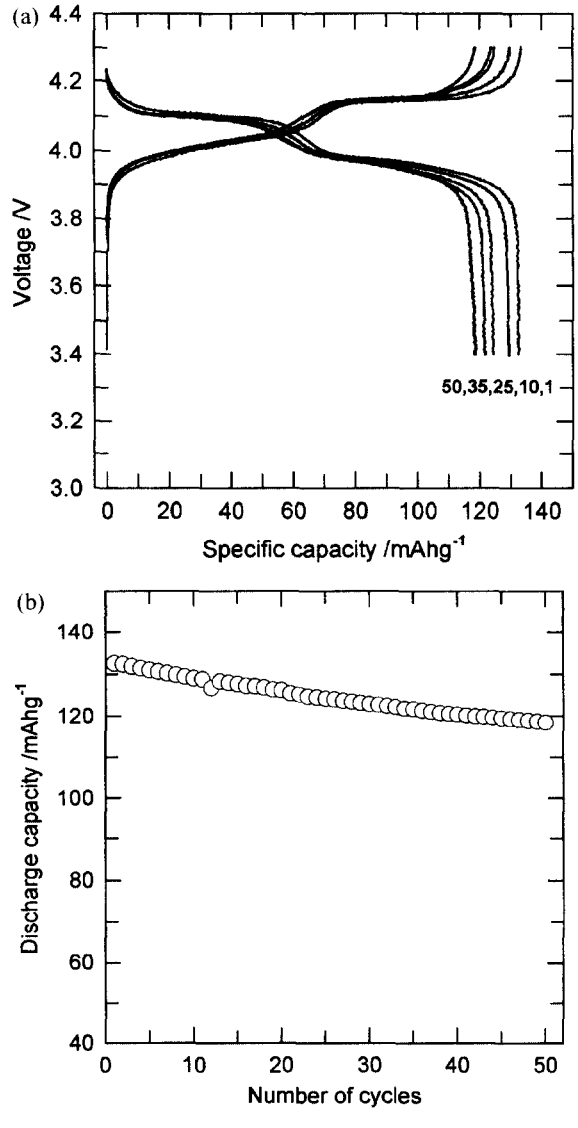

Fig. 9. (a) Cycling charge/discharge curves and (b) variation of specific discharge capacity with number of cycles for the Li/polymer electrolyte/$LiMn_2O_4$ cells. Cycling was galvanostatically carried out at constant charge/discharge current density of 0.1 mA/cm^2 between 3.0 and 4.3 V.

Fig. 9 shows the charge/discharge curves and discharge capacities with number of cycles for the Li/polymer electrolyte/$LiMn_2O_4$ cell using $LiMn_2O_4$ powders calcined at 800 °C. The cells were cycled between cut-off voltages of 3.4 and 4.3V at a constant current density of 0.1 mA/cm^2. The Li/polymer electrolyte/$LiMn_2O_4$ cells show that the discharge curves have two distinct plateaus which are the characteristics of the manganese-oxide spinel structure [Xia et al., 1996]. The cell polarization during 1st cycle which means half of the difference in voltage between the charge and discharge curves at 74 mAh/g was low (0.07 V) compared to the one of 0.065 V reported by author, which have good cyclability [Sun et al., 1997], and increased with cycling. The Li/polymer electrolyte/$LiMn_2O_4$ cell initially delivered 132 mAh/g. The discharge capacity slowly decreased with cycling and remained about 119 mAh/g up to 50th cycles. It has been well known that the capacity fading is resulting from Mn dissolution [Jang et al., 1996; Xia et al., 1996]. Although Mn dissolution in the gel-type polymer electrolyte system is not so severe as that in liquid electrolyte, its contribution to the capacity loss is not negligible. It can be expected that the reduced capacity is attributable to other contributions besides Mn dissolution. The capacity fading of the Li/polymer electrolyte/$LiMn_2O_4$ cell may be related to the deterioration of interfacial contacts ($LiMn_2O_4$/conducting carbon/PAN) for the composite cathode as a result of $LiMn_2O_4$ lattice change of the during charge/discharge cycling [Sun et al., 1997; Jiang et al., 1996]. A significant strain on the interface of the composite cathode is

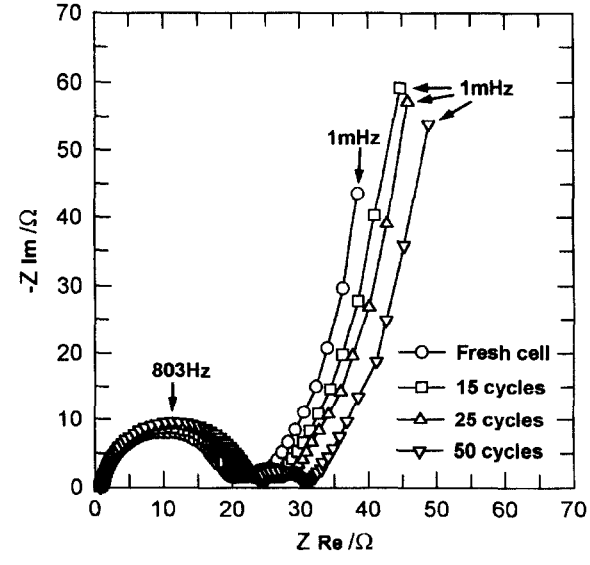

Fig. 10. Typical Nyquist plots obtained from the cell Li/polymer electrolyte/$LiMn_2O_4$ electrode in charge state with respect to the number of cycles.

believed to degrade the electrical contact between the surfaces of the insertion particles, and hence to decrease the capacity of the cathode during repeated charge/discharge cycling.

In order to investigate the origin of observed capacity fading, we studied the interfacial resistance behavior between polymer electrolyte and composite $LiMn_2O_4$ electrode with cycling. Fig. 10 shows the A.C. impedance spectra of the Li/polymer electrolyte/$LiMn_2O_4$ cell (three-electrode electrochemical cell type) after various cycling tests at fully charged state. The impedance spectra consist of two semicircles in the high and intermediate frequency ranges, and a line inclined at constant angle to the real axis in the low-frequency range. The two semicircles in the higher frequency range may be due to the contact resistance at the composite cathode and the reaction at the interface of the electrolyte/oxide electrode ; and the inclined line in the lower frequency range is attributed to Warburg impedance that is associated with lithium ion diffusion through the oxide electrode. It has been reported that the magnitude of the high-frequency semicircle increased with increasing oxide-electrode mass and it decreased with increasing amounts of carbon used as a conducting agent [Choi et al., 1995]. This result suggests that the high-frequency semicircle represents particle-to-particle contact resistance and capacitance within the oxide particles, and that the intermediate frequency arc is related to the reaction at polymer electrolyte/cathode (oxide electrode) interface. As the number of cycles increased, the magnitude of the high-frequency and intermediate-frequency arcs increased monotonically with cycling, indicating deterioration of contacts for the cathode and the increase of the interfacial resistance between cathode and polymer electrolyte as a result of volume changes of the cathode during charge/discharge cycling, respectively. From this result, it can be inferred that the capacity fading for the cell Li/polymer electrolyte/$LiMn_2O_4$ may be related to the deterioration of contact within the oxide electrode and the increase of the interfacial resistance at polymer electrolyte/cathode as well as Mn dissolution. The interfacial resistance between Li metal and polymer electrolyte is also thought to be another factor for determining the cycling characteristics of Li/polymer electrolyte/$LiMn_2O_4$ cell. It is necessary to study the electrochemical characteristics between Li metal and polymer electrolyte in the near future.

CONCLUSIONS

Spinel $LiMn_2O_4$ powders with submicron, monodispersed, and highly homogeneous particles were synthesized by a sol-gel method using an aqueous solution of metal acetate containing glyoxylic acid as a chelating agent. The physicochemical properties of the $LiMn_2O_4$ powders have been investigated as a function of the calcination temperature and glyoxylic acid quantity. It was seen that as the calcination temperature was increased whereas the crystallinity was increased, the specific surface area of $LiMn_2O_4$ powders was decreased. The $LiMn_2O_4$ powders with a wide variety of physicochemical properties could be controlled by simply varying the pyrolysis condition and glyoxylic acid quantity. The glyoxylic acid-assisted $LiMn_2O_4$ powders delivered an initial capacity of 132 mAh/g, and showed an excellent rechargeability in the Li/polymer electrolyte/$LiMn_2O_4$ cell. The capacity fading of the cell is related to the deterioration of contact within the oxide electrode and the increase of the interfacial resistance at polymer electrolyte/cathode as well as Mn dissolution.

REFERENCES

Bruce, P. G. and Krok, F., "Characterization of the Electrode/Electrolyte Interfaces in Cells of the Type Li/PEO-$LiCF_3SO_3$/V_6O_{13} by ac Impedance Methods," *Solid State Ionics*, **36**, 171 (1989).

Choi, Y.-M., Pyun, S.-I., Bae, J.-S. and Moon, S.-I., "Effects of Lithium Content on the Electrochemical Lithium Intercalation Reaction into $LiNiO_2$ and $LiCoO_2$ Electrodes," *J. Power Sources*, **56**, 15 (1995).

Fauteux, D., "Lithium Electrode/PEO-Based Polymer Electrolyte Interface Behavior Between 60 and 120°C," *J. Electrochem. Soc.*, **135**, 2231 (1988).

Guyomard, D. and Tarascon, J. M., "The Carbon/$Li_{1+x}Mn_2O_4$ System," *Solid State Ionics*, **69**, 222 (1994).

Gao, Y. and Dahn, J. R., "Synthesis and Characterization of $Li_{1+x}Mn_{2-x}O_4$ for Li-Ion Battery Applications," *J. Electrochem. Soc.*, **143**, 100 (1996).

Hiratani, M., Miyauchi, K. and Kudo, T. "Electrode Reaction at the Interface Between Lithium Anode and a Solid Electrolyte," *Solid State Ionics*, **28-30**, 1431 (1988).

Jang, D. H., Shin, S. J. and Oh, S. M., "Dissolution of Spinel Oxides and Capacity Losses in 4 V $Li/Li_xMn_2O_4$," *J. Electrochem. Soc.*, **143**, 2204 (1996).

Jiang, Z. and Abraham, K. M., "Preparation and Electrochemical Characterization of Micron-Sized Spinel $LiMn_2O_4$," *J. Electrochem. Soc.*, **143**, 1591 (1996).

Koksbang, R., Olsen, I. I., Tonder, P. E., Knudsen, N. and Fauteux, D., "Polymer Electrolyte Lithium Batteries Rechargeability and Positive Electrode Degradation : An AC Impedance Study," *J. Appl. Electrochem.*, **21**, 301 (1991).

Lessing, P. A., "Mixed-Cation Oxide Powders via Polymeric Precursors," *Ceram. Bull.*, **68**, 1002 (1989).

Macklin, W. J., Neat, R. J. and Powell, R. J., "Performance of Lithium-Manganese Oxide Spinel Electrodes in a Lithium Polymer Electrolyte Cell," *J. of Power Sources*, **34**, 39 (1991).

Masquelier, C., Tabuchi, M., Ado, K., Kanno, R., Kobayashi, Y., Maki, Y., Nakamura, O. and Goodenough, B., "Chemical and Magnetic Characterization of Spinel Materials in the $LiMn_2O_4$-$Li_2Mn_4O_9$-$Li_4Mn_5O_{12}$ System," *J. Solid State Chem.*, **123**, 255 (1996).

Ratnakumar, B. V., Di Stefano, S. and Bankston, C. P., "A.C. Impedance of Niobium Triselenide Cathode in Secondary Lithium Cells," *J. Appl. Electrochem*, **19**, 813 (1989).

Steele, B. C. H., Lagos, G. E., Spurdens, P. C., Forsyth, C. and Foord, A. D., "Behaviour of $Li_xV_6O_{13}$ and Li_xTiS_2 Composite Electrodes Incorporating Polyethylene Oxide Based Electrolytes," *Solid State Ionics*, **9&10**, 391 (1983).

Sun, Y.-K., Oh, I.-H. and Kim, K. Y., "Synthesis of Spinel $LiMn_2O_4$ by the Sol-Gel Method for a Cathode-Active Material in Lithium Secondary Batteries," *Ind. & Eng. Chem. Res.*, **36**, 4839 (1997).

Sun, Y.-K., "Synthesis and Electrochemical Studies of Spinel $Li_{1.03}Mn_2O_4$ Cathode Materials Prepared by a Sol-Gel Method for Lithium Secondary Batteries," *Solid State Ionics*, **100**, 115 (1997).

Xia, Y., Zhou, Y. and Yoshio, M., "Capacity Fading on Cycling of 4 V $Li/LiMn_2O_4$ Cells," *J. Electrochem. Soc.*, **144**, 2593 (1997).